Electronic Supplementary Material (ESI) for Catalysis Science & Technology.

Microwave-induced synthesis of a bimetallic charge-transfer metal organic framework: A promising host for the chemical fixation of CO_2 via cyclic carbonate synthesis

Jintu Francis Kurisingal,[a] Robin Babu,[a] Seol-Hee Kim,[a] YiXin Li,[a] Jong-San Chang,[b] Sung June Cho[c] and Dae-Won Park[a*]

(a) Division of Chemical and Biomolecular Engineering, Pusan National University, Busan, 46241, Korea

(b)Korea Research Institute of Chemical Technology, Daejeon, 34101, Korea

(c)Department of Applied Chemical Engineering, Chonnam National University, Kwangju 500-757, Korea

Experimental Section

Chemicals

$NiCl_2.6H_2O$ (Alfa Aesar), $CoCl_2.6H_2O$ (Sigma Aldrich), BDC (Sigma Aldrich), ECH, all epoxides (Sigma-Aldrich), toluene (Sigma-Aldrich), dichloromethane (Sigma-Aldrich), and deionized water were used for all catalyst syntheses and activity experiments.

Microwave-assisted synthesis of Ni-Co-MOF

The rapid synthesis of Ni-Co-MOF was performed in a multimode microwave reactor (KMIC-2 KW) having a continuously adjustable power source (range 0–2 kW) with a three-stub tuner, operated at a frequency of 2.450 GHz. In this method, 0.089 g of $NiCl_2.6H_2O$ (0.375 mmol) and 0.089 g of $CoCl_2.6H_2O$ (0.375 mmol) was dissolved in a 100 mL beaker containing 15 mL deionized water and stirred for 5 min. Subsequently, 0.125 g of BDC (0.75 mmol) was dissolved in another 100 mL beaker containing 15 mL deionized water. After that, the 15 mL BDC solution is added to the above mentioned 15 mL metal solution. The mixed solution was transferred to a 40 mL Pyrex glass reactor tube after sonicating for 10 min. The glass reactor tube was sealed carefully and irradiated at a microwave power of 200 W, providing a temperature of 90 °C (the desired temperature is achieved with in 2 min), for 10 min. The reaction mixture was allowed to cool to room temperature, and the crystals produced were washed with methanol three times, centrifuged at 7000 rpm, and then dried in a vacuum oven at 60 °C overnight.

Solvothermal synthesis of Ni-Co-MOF

In a typical synthesis, 0.089 g of $NiCl_2.6H_2O$ (0.375 mmol) and 0.089 g of $CoCl_2.6H_2O$ (0.375 mmol) was dissolved in a 100 mL beaker containing 15 mL deionized water and stirred for 5 min.

Subsequently, 0.125 g of BDC (0.75 mmol) was dissolved in another 100 mL beaker containing 15 mL deionized water. After that, the 15 mL BDC solution is added to the above mentioned 15 mL metal solution. Finally, the resultant solution was stirred for 10 min and transferred to a 50 mL Teflon-lined autoclave and then heated at 140 °C (3 ˚C/ min) for 48 h under airtight conditions.[1] After cooling, the solid product was centrifuged at 7000 rpm for 10 min. The resultant solid was then washed with methanol three times and dried in a vacuum oven at 60 °C overnight.

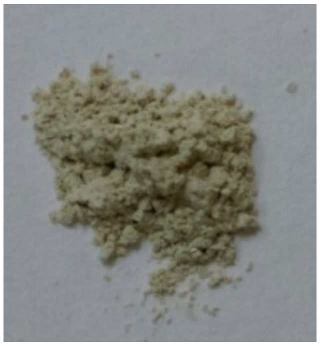

Ni-Co MOF

Microwave-assisted synthesis of Ni-MOF and Co-MOF

In a typical synthesis, 0.178 g of $NiCl_2.6H_2O$ (0.75 mmol) (for Ni-MOF) or 0.178 g of $CoCl_2.6H_2O$ (0.75 mmol) (for Co-MOF) was dissolved in 15 mL deionized water and stirred for 5 min. Subsequently, 0.75 mmol BDC was dissolved in a 100 mL beaker containing 15 mL deionized water and stirred for 5 min. Subsequently, 0.125 g of BDC (0.75 mmol) was dissolved in another 100 mL beaker containing 15 mL deionized water. After that, the 15 mL BDC solution is added to the above mentioned 15 mL metal solution. The mixed solution was transferred to a 40 mL Pyrex glass reactor tube after sonicating for 10 min. The glass reactor tube was sealed carefully and irradiated at a microwave power of 200 W, providing a temperature of

90 °C (the desired temperature is achieved with in 2 min), for 10 min. The reaction mixture was allowed to cool to room temperature, and the crystals produced were washed with methanol three times, centrifuged at 7000 rpm, and then dried in a vacuum oven at 60 °C overnight.

Ni-MOF

Co-MOF

CO_2-epoxide cycloaddition reactions

All the cycloaddition reactions were conducted in a 25 mL stainless steel autoclave reactor charged with the requisite amount of catalyst, epoxide, and cocatalyst and subjected to magnetic stirring at 500 rpm. The reactions were conducted under pre-decided CO_2 pressures at different temperatures. After finishing the reaction, the stirrer was turned off, the reactor was cooled to < 5 °C using an ice-bath, and the excess CO_2 was vented. The internal standards toluene and dichloromethane were added to the product mixture, which was then filtered. The yields were then determined using a gas chromatographer (Agilent technologies, HP 6890 A) fitted with a 30 m × 0.25 μm capillary column (HP-5) and a flame ionization detector.

^{1}H NMR Details of Epichlorohydrin Carbonates

(300 MHz, CDCl3) δ 4.96−4.91 (m, 1H, OCH), 4.53−4.47 (m, 1H, CH2), 4.31−4.26 (m, 1H, CH2), 3.78−3.61 (m, 2H, CH2Cl).

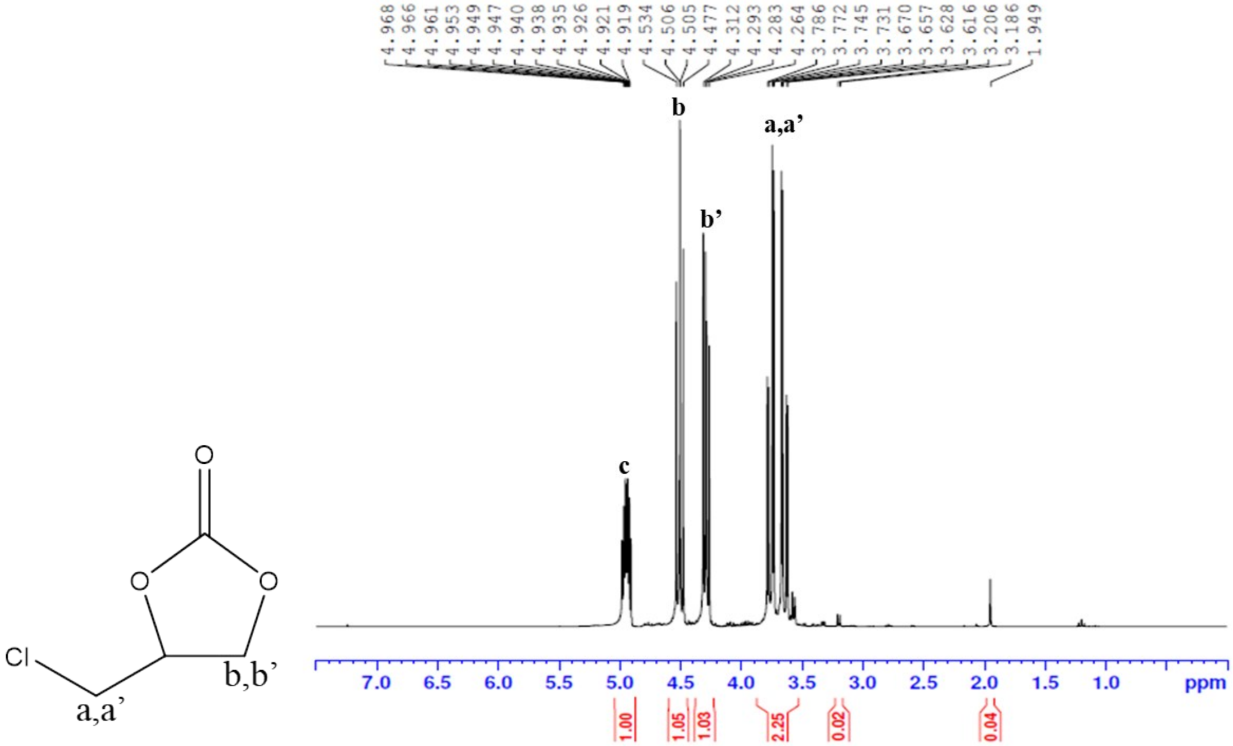

Characterization

Powder X-ray diffraction (PXRD) patterns were obtained in XPERT-PRO diffractometer system using 40 kV CuKα radiation (30 mA) with minimum step size 2θ= 0.001 and scan step time of 0.9000 s. Elemental analysis (EA) was performed using a Vario-Micro cube system, Germany. 1.8 mg of catalyst was subjected to analysis at 1150°C with benzoic acid (for Oxygen) and sulfanilic acid (for Carbon and Hydrogen) as the standards. The weight percentage of the metal in the catalyst were obtained from inductively coupled plasma atomic emission spectroscopy

(ICP-OES) analysis using an Activa, JY Horiva (1.5 kW, 40.68 MHz, 130–800 mm) fitted with a monochromatic HDD and a polychromatic PMT detector. Thermogravimetric analysis (TGA) was conducted with SDT Q600 apparatus. 3.13 mg of sample was subjected to analysis at a heating rate of 10˚C/ min from 50˚C to 600 ˚C under a nitrogen flow of 100ml/ min. Fourier-transform infrared (FT-IR) spectra of the catalyst were recorded on an AVATAR 370 Thermo Nicolet spectrophotometer at a resolution of 4 cm^{-1}. Field emission scanning electron microscopy (FE-SEM, Zeiss supra 40 VP) images were observed using S-4200 field emission scanning electron microscope at 5.00 kV. The XPS analysis of the catalysts was carried out using theta probe AR-XPS system (Thermo Fisher Scientific (U.K)). The instrument used the X-ray source of monochromated Al Kα (hv= 1486.6 eV) having the energy of 150W. CO_2 and NH_3 TPD profiles were acquired with a chemisorption analyzer (BEL-CAT) as follows. Before the measurements, 0.053 g of the sample was activated in He (30 mL min^{-1}) at 280 °C for 1 h. The sample was subsequently exposed to the pulses of CO_2 or NH_3 in Heat 40 °C for 1 h. The sample was then flushed with He (30 mL min^{-1}) for 1 h. TPD measurements were carried out by raising the temperature from 40 to 280 °C at a heating rate of 5 °C min^{-1}. The textural properties of the catalyst were analyzed by recording an N2 adsorption isotherm at 77 K with a BET apparatus (Micromeritics ASAP 2020). The specific surface area was determined using the BET model equation.

Experimental method of XAFS

X-ray absorption fine spectroscopy (XAFS) data of the MOF samples over Co K edge, 7729 eV in ambient condition was collected with *R*-XAS instrument (Rigaku, Japan) operating at 20 kV and 15 mA with a W filament using Ge (240) crystal as monochromator. The step and duration time for extended X-ray absorption fine structure (EXAFS) were 2.0 eV and 100 s, respectively.

For XAFS analysis, Artemis implemented in in Demeter program package (0.9.25) was utilized after the data processing using Athena.[2] The background removal was performed to extract XAFS signal using AUTOBK program for R_{bkg}=0.1 nm and subsequently the corresponding XAFS data in k space was fourier transformed with the Kaiser-Bessel window function, 10 nm^{-1} after k^3 weighting to amplify the high k information.[3] The range for fourier transformation for samples, Δk were 20 – 120 nm^{-1} or 2 - 12 $\mathrm{Å}^{-1}$. The phase shifts and amplitude functions of the reference was generated using *Feff* 6L.[4] The curve fitting range in r space, Δr was varied depending on the sample. The number of independent point of the data for the curve fit, N_{idp} determined from Nyquist theorem was always larger than the number of variable, providing the sufficient degree of freedom, N_{var}. The scattering path from the possible model structure was obtained from the *Feff* calculation. Only scattering with large contribution, single scattering due to Co atom were included in the multi-shell fitting. The manybody reduction factor, S_0^2 for Co, 0.9 was obtained from the curve fit of the XAFS data of Co foil under the same condition and utilized further in the curve fit of the sample. The statistical quality of the curve fit or proposed model was determined from the R-factor available in the refinement.

Reference

1. Zhao, et al. *Nat. Energy* **2016,** *1*, 16184.
2. B. Ravel, M. Newville, *J. Synch. Rad.* **2005**, *12*, 537−541.
3. M. Newville, P. Livins, Y. Yacoby, J. J. Rehr, E. A. Stern, *Phys. Rev. B* **1993**, *47*, 14126-14131.
4. J. J. Rehr, R. C. Albers, S. I. Zabinsky, *Phys. Rev. Lett.* **1992**, *69*, 3397-3400.

Table S1 Result of data analysis of X-ray absorption fine structure obtained at K edge.

Atomic parameters	Crystal data on Co-MOF[a]	XAFS refinement[b]		
		Co-MOF	Ni-Co MOF[e]	Ni-MOF[f]
CN of $Co_{1/2}$-O_1	2/2	2	2	4
R of $Co_{1/2}$-O_1 (nm)	0.198/0.205	0.210±0.016	0.195±0.018	0.202±0.015
σ^2 of $Co_{1/2}$-O_1 (pm^2)		47±127	33±212[g]	164±131
CN of $Co_{1/2}$-O_2	2/2	2	2	2
R of $Co_{1/2}$-O_2 (nm)	0.215/0.211	0.213±0.010	0.207±0.005	0.204±0.006
σ^2 of $Co_{1/2}$-O_2 (pm^2)		116±389[g]	-3±227[h]	34±58
CN of $Co_{1/2}$-O_3	2/2	2	2	
R of $Co_{1/2}$-O_3 (nm)	0.220/0.214	0.233±0.038	0.219±0.009	
σ^2 of $Co_{1/2}$-O_3 (pm^2)		116±389[g]	33±212[g]	
CN of $Co_{1/2}$-C_1	4		5	
R of $Co_{1/2}$-C_1 (nm)	0.298		0.291±0.016	
σ^2 of $Co_{1/2}$-C_1 (pm^2)			231±29	
CN of Co_1-Co_1	2	2	2	2
R of Co_1-Co_1 (nm)	0.331	0.322±0.004	0.320±0.008	0.320±0.009
σ^2 of Co_1-Co_1 (pm^2)		96±46	117±99	114±97
CN of Co_1-C_2	4	4	4	4
R of Co_1-Co_2 (nm)	0.355	0.355±0.010	0.354±0.007	0.349±0.003
σ^2 of Co_1-Co_2 (pm^2)		208±114	129±77	131±76
N_{idp}[c]		23.8	23.8	23.1
N_{var}[d]		19	21	20
ΔE (eV)		4.5±2.5	-1.8±5.0	-3.1±5.3
R-factor (%)		3.8	3.1	3.6

[a] Crystallographic data obtained from reference no. 4. There are two asymmetric Co, Co_1 and Co_2. The two different distances in the first shell were given.

[b] For the refinement, only the XAFS data obtained at Co K edge was utilized because the difference between Ni and Co edge is 700 eV and then the XAFS signal at Co K edge can interfere the data analysis of XAFS obtained at Ni K edge. The single scattering contributions up to 0.4 nm except from C atom have been included to account the radial distribution function while the coordination number in each shell was fixed. The contribution from the multiple scattering can be ignored because it was weak relatively and diffuse compared to the single scatter like Co

[c] Number of independent point can be used for the refinement, which can be calculated from the Nyquist theorem using given Δr, $0.1 \le r$ (nm) ≤ 0.4 and Δk range, $20 \le k$ (nm^{-1}) ≤ 120, respectively.

[d] Number of variable used in the refinement for XAFS data analysis.

[e] The single scattering contribution from C atom has been included for the refinement where it was strong relatively and also the corresponding coordination number was increased to take into account of the multiple scattering effect at the same distance. The Co scatter was a mixture of Co and Ni but it was considered as Co atom only because of only an electron difference between Co and Ni.

[f] The two oxygen contribution in the first shell was merged because each distances were indistinguishable in the refinement. Co atom was replaced to Ni atom as X-ray absorber and scatter, respectively.

[g] The Debye-Waller factor of two Co-O shell was assumed to be the same for the same functional group.

[h] The Debye-Waller factor was zero practically considering the estimated error.

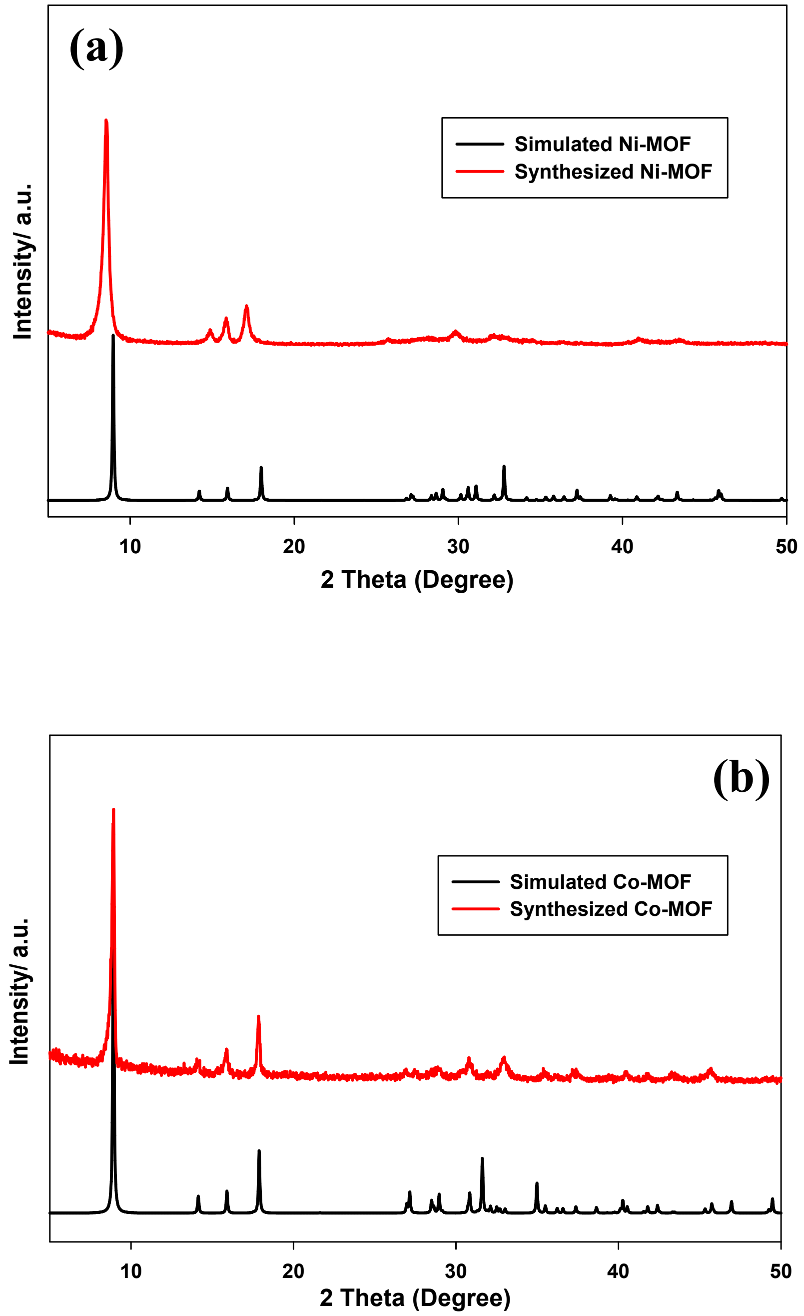

Fig. S1 PXRD patterns of (a) Ni-MOF and (b) Co-MOF catalysts compared to the simulated single crystal patterns.

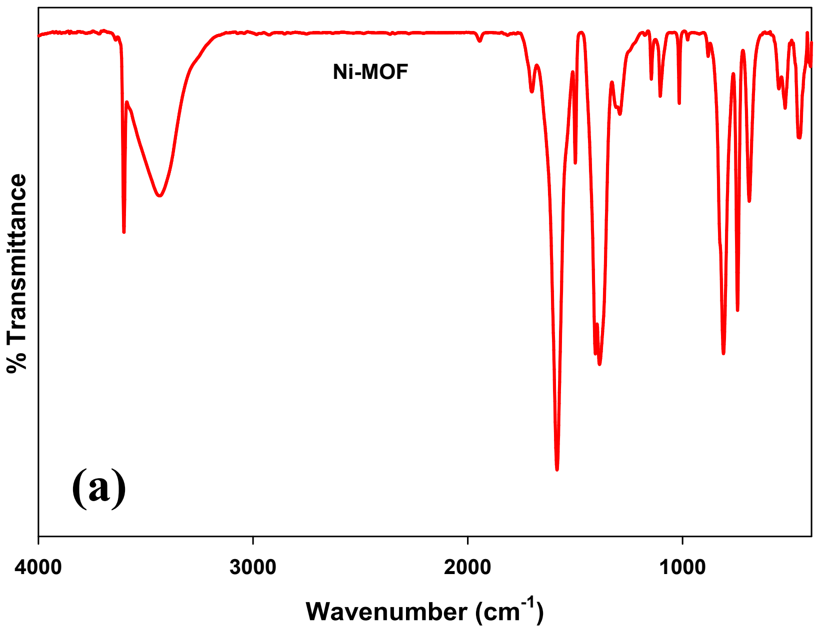

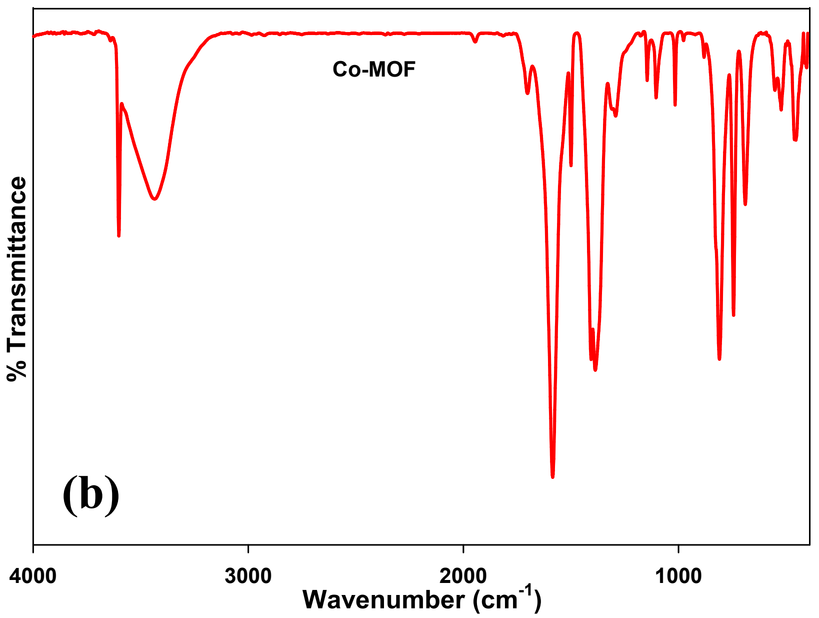

Fig. S2 FT-IR spectra of (a) Ni-MOF and (b) Co-MOF.

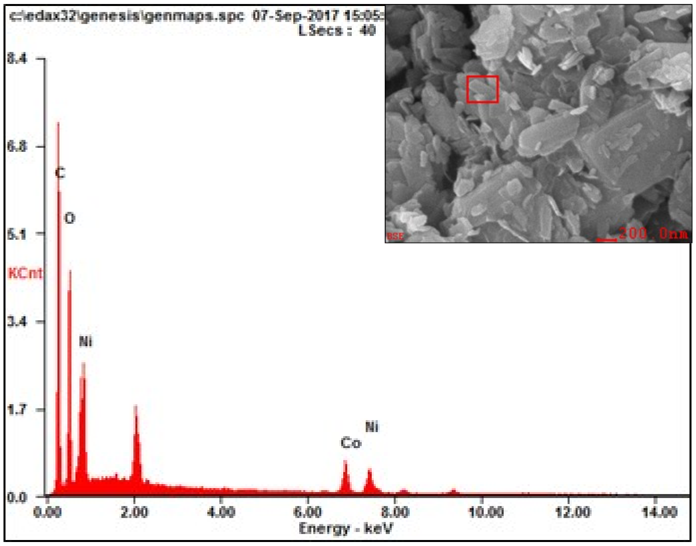

Element	***Wt%***	***At%***
CK	41.71	63.64
OK	21.82	24.99
CoK	18.21	05.66
NiK	18.26	05.70
Matrix	Correction	ZAF

Fig. S3 SEM-EDS analysis of Ni-CO MOF(M).

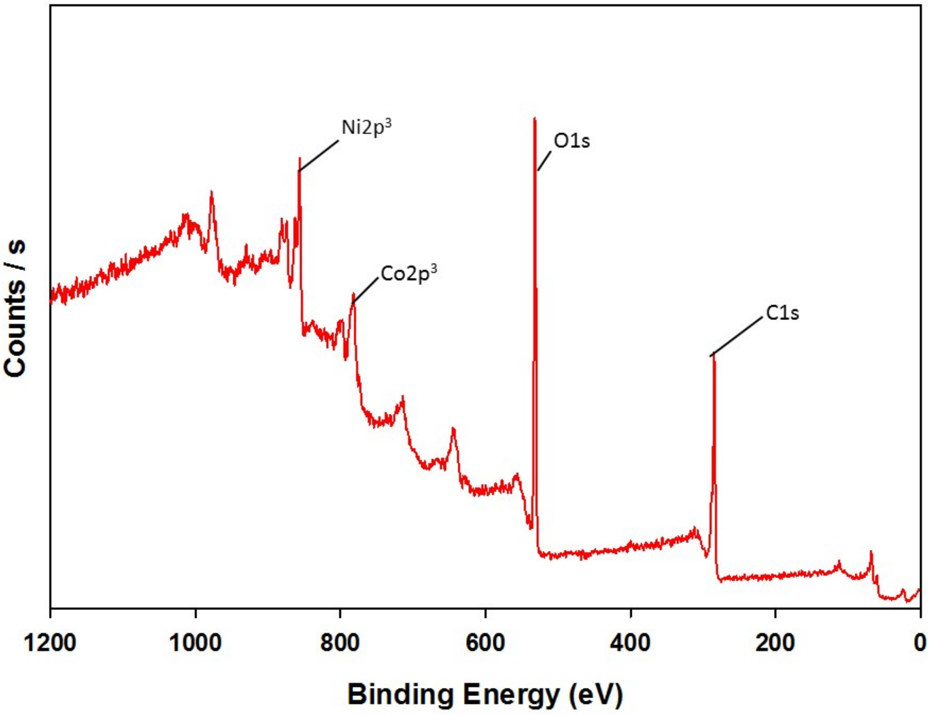

Fig. S4 XPS spectra of Ni-Co MOF(M).

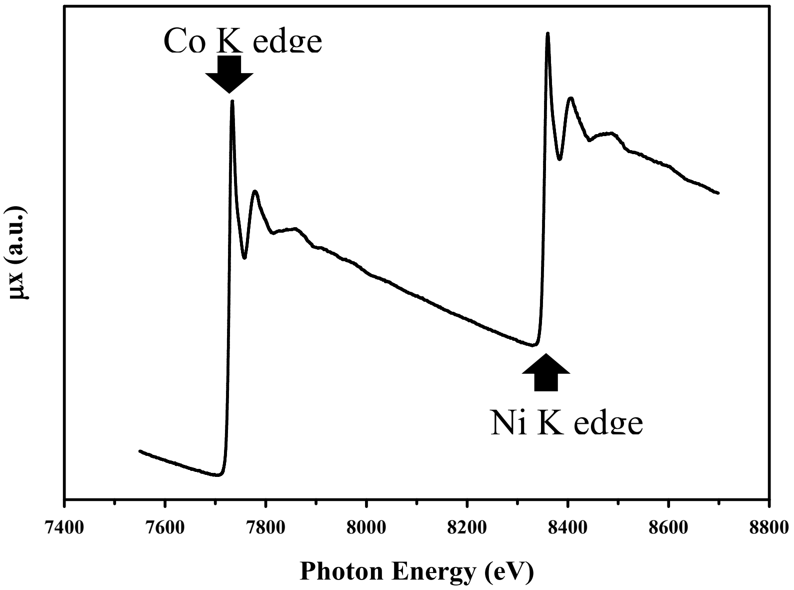

Fig. S5 X-ray absorption spectrum of Ni-Co MOF at Co K edge.

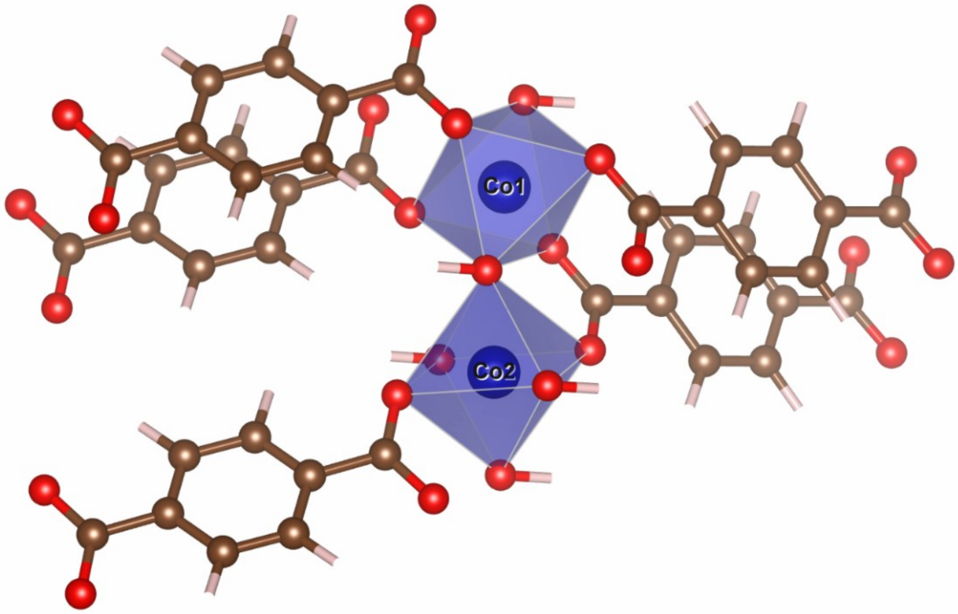

Fig. S6 Crystal structure of Co(BDC)$_2$

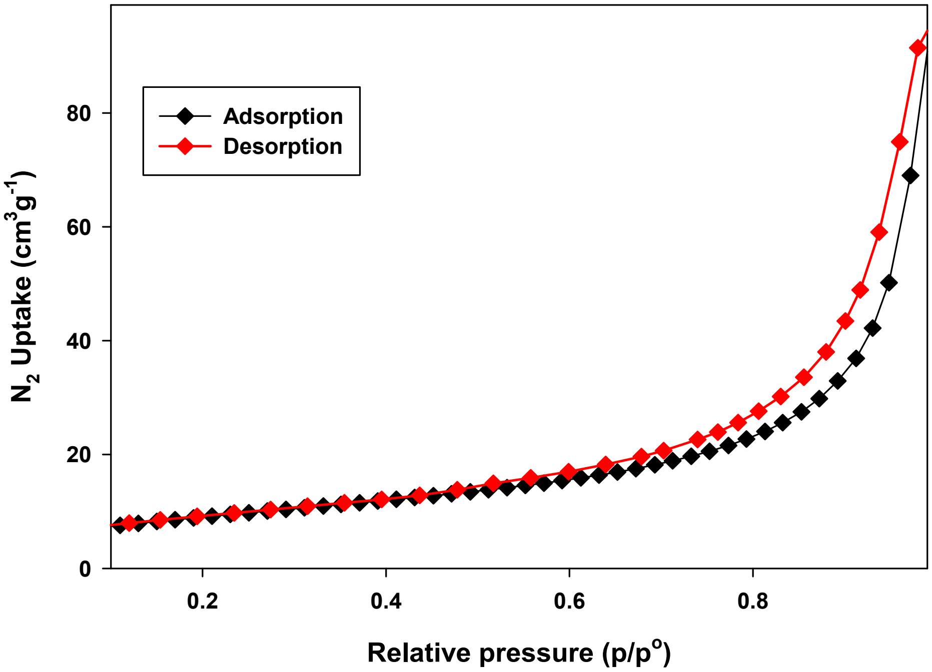

Fig. S7 N_2 adsorption-desorption isotherm of Ni MOF.

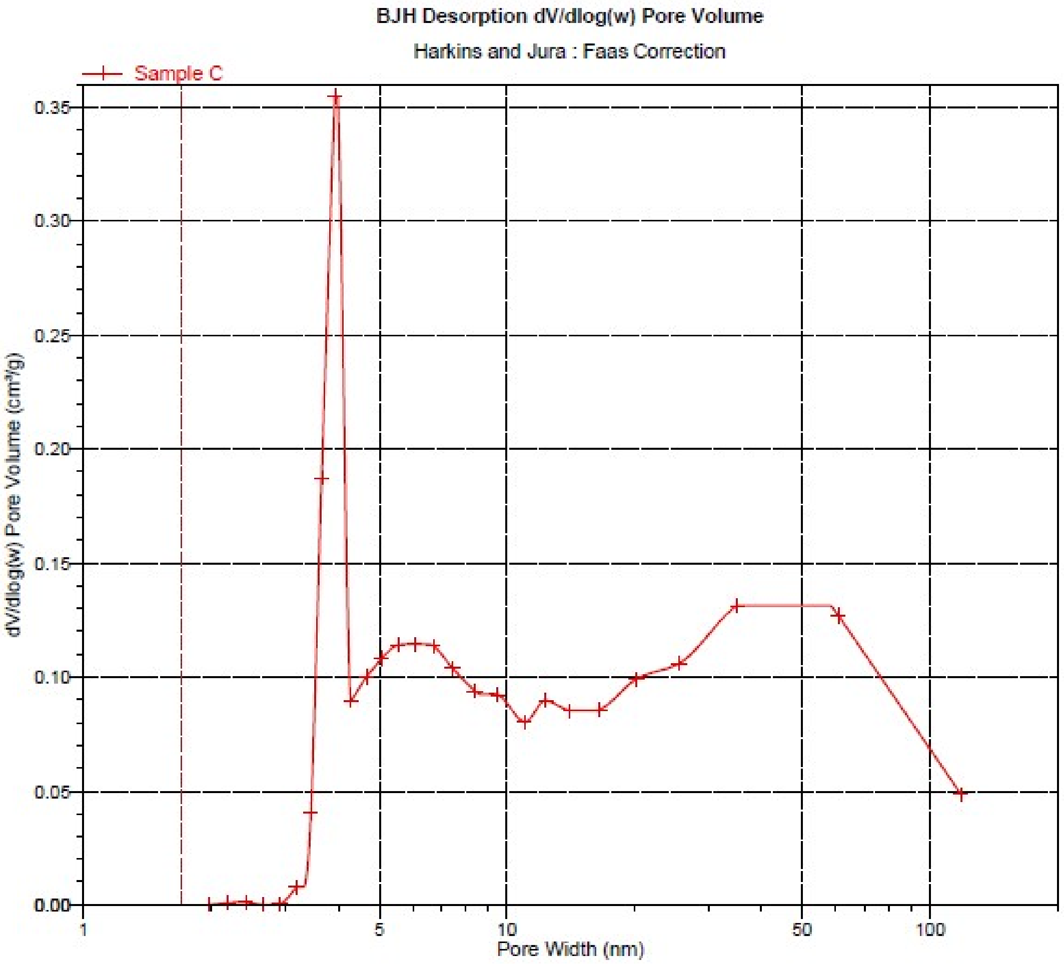

Fig. S8 Pore size distribution of Ni-Co MOF.

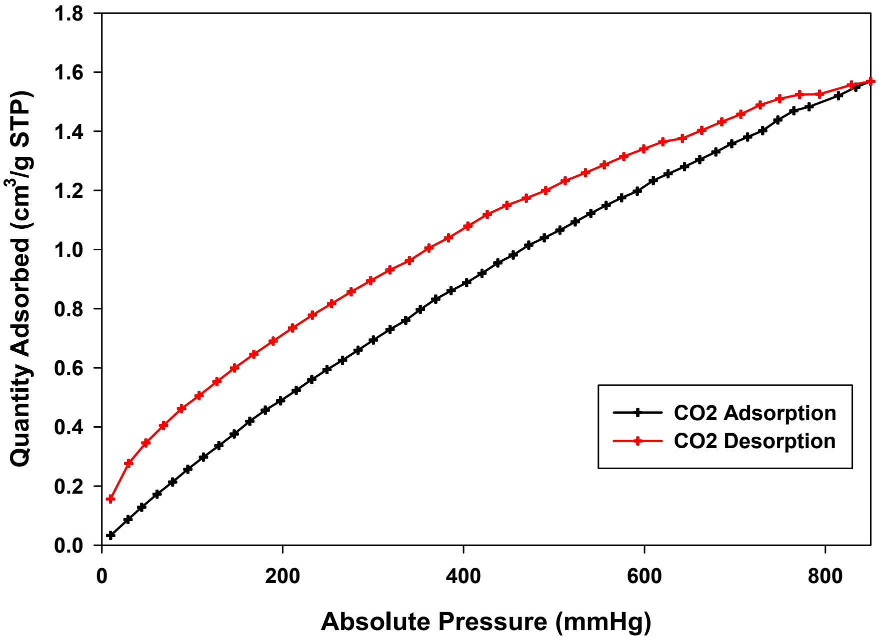

Fig. S9 CO_2 adsorption-desorption analysis of Ni-Co MOF(M) at 25 ˚C.

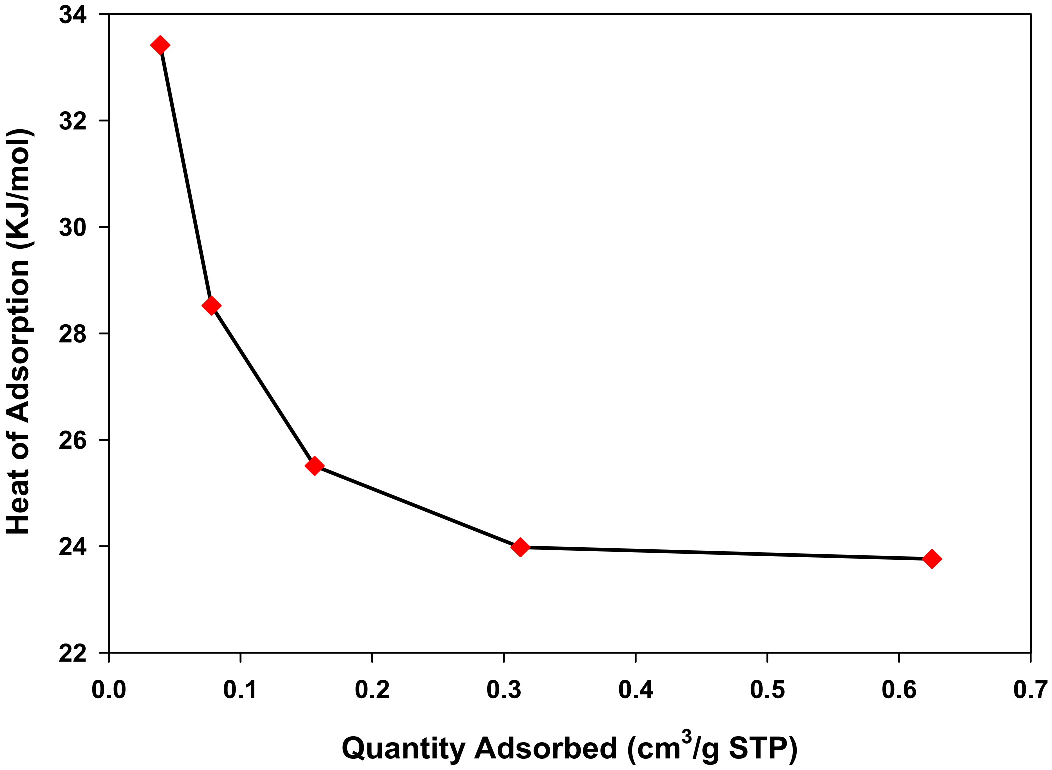

Fig. S10 Heat of adsorption plot of Ni-Co MOF(M).

No.	Start time (sec)	End time (sec)	Time width (sec)	Peak position (sec)	Peak position (‹C)	Area (count)	mmol	mmol/g	log(W/F)+3
1	3830	5635	1806	4648	117.5	141,071	0.292	5.438	
2	5636	7554	1919	6544	275.2	442,915	0.917	17.074	

(a)

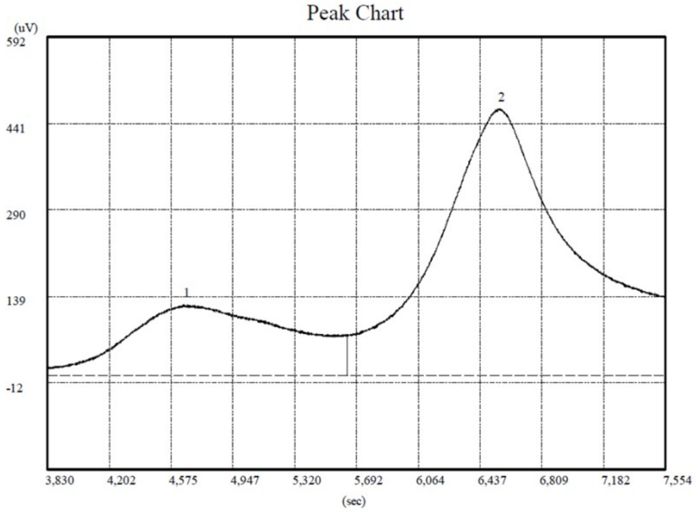

No.	Start time (sec)	End time (sec)	Time width (sec)	Peak position (sec)	Peak position (‹C)	Area (count)	mmol	mmol/g	log(W/F)+3
1	3829	5695	1867	5694	202.1	203,913	0.005	0.082	
2	5696	7562	1867	6693	267.1	1,444,850	0.034	0.584	

(b)

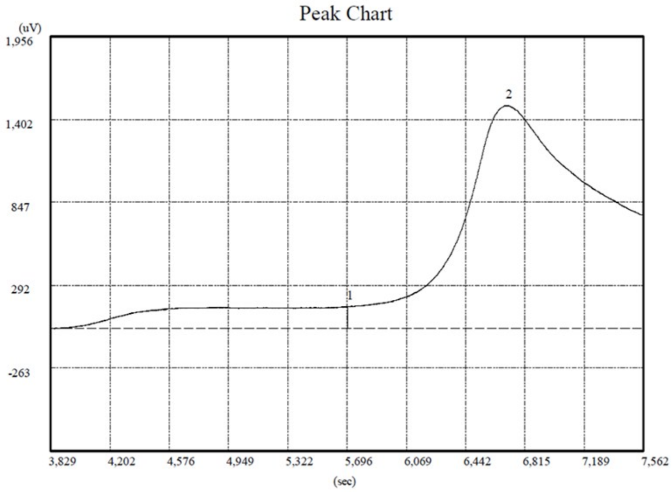

Fig. S11 TPD plots of (a) acidic and (b) basic sites in Ni-Co MOF(M).

No.	Start time (sec)	End time (sec)	Time width (sec)	Peak position (sec)	Peak position (‹C)	Area (count)	mmol	mmol/g	log(W/F)+3
1	3786	5539	1754	4542	113.6	41,655	0.086	1.658	
2	5540	7528	1989	6706	276.9	119,027	0.246	4.738	

(a)

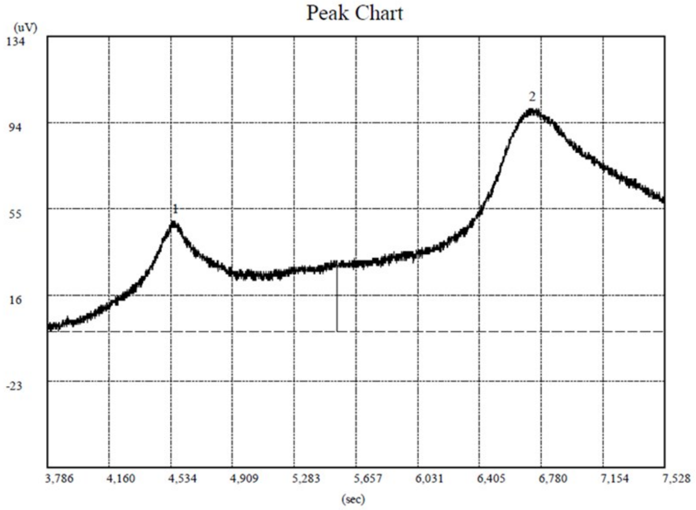

No.	Start time (sec)	End time (sec)	Time width (sec)	Peak position (sec)	Peak position (‹C)	Area (count)	mmol	mmol/g	log(W/F)+
1	3794	4718	925	4388	101.1	340,649	0.008	0.144	
2	4719	7422	2704	5125	164.4	1,116,907	0.026	0.471	

(b)

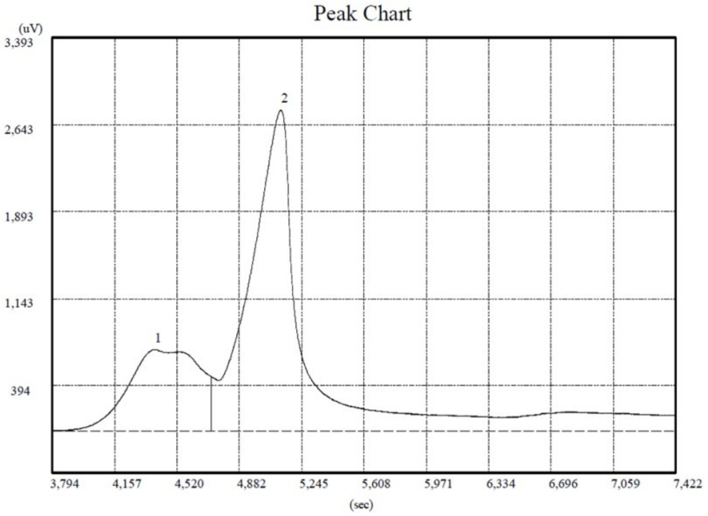

Fig. S12 TPD plots of (a) acidic and (b) basic sites in Ni-MOF.

No.	Start time (sec)	End time (sec)	Time width (sec)	Peak position (sec)	Peak position (‹C)	Area (count)	mmol	mmol/g	log(W/F)+3
1	3809	5818	2010	4521	111.6	49,035	0.102	1.839	
2	5819	7471	1653	6736	274.5	92,431	0.191	3.466	

(a)

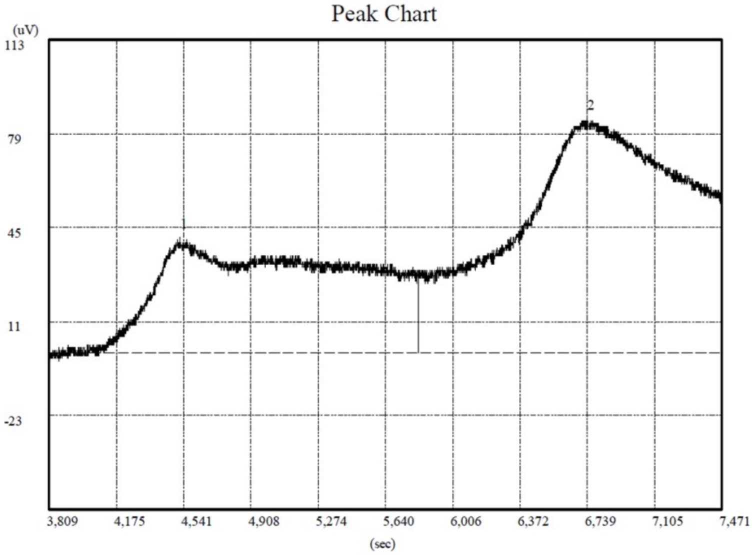

No.	Start time (sec)	End time (sec)	Time width (sec)	Peak position (sec)	Peak position (‹C)	Area (count)	mmol	mmol/g	log(W/F)+3
1	3830	4823	994	4441	96.7	248,124	0.006	0.104	
2	4824	7344	2521	5202	156.9	830,567	0.020	0.349	

(b)

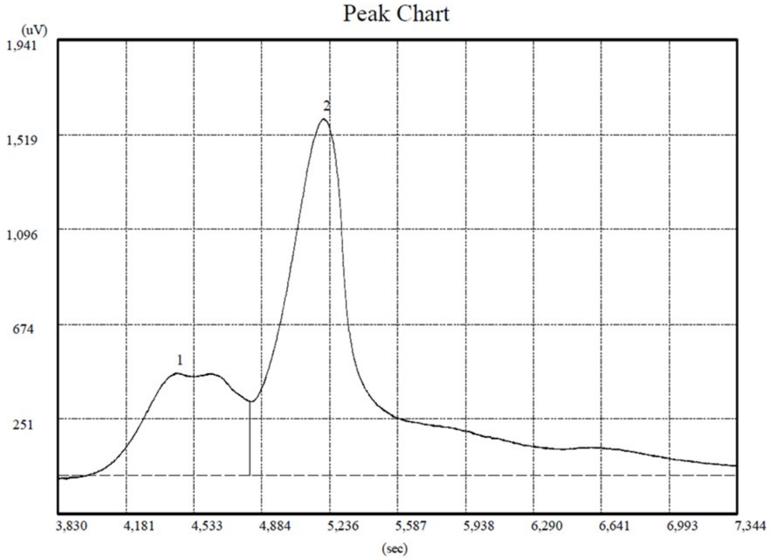

Fig. S13 TPD plots of (a) acidic and (b) basic sites in Co-MOF.

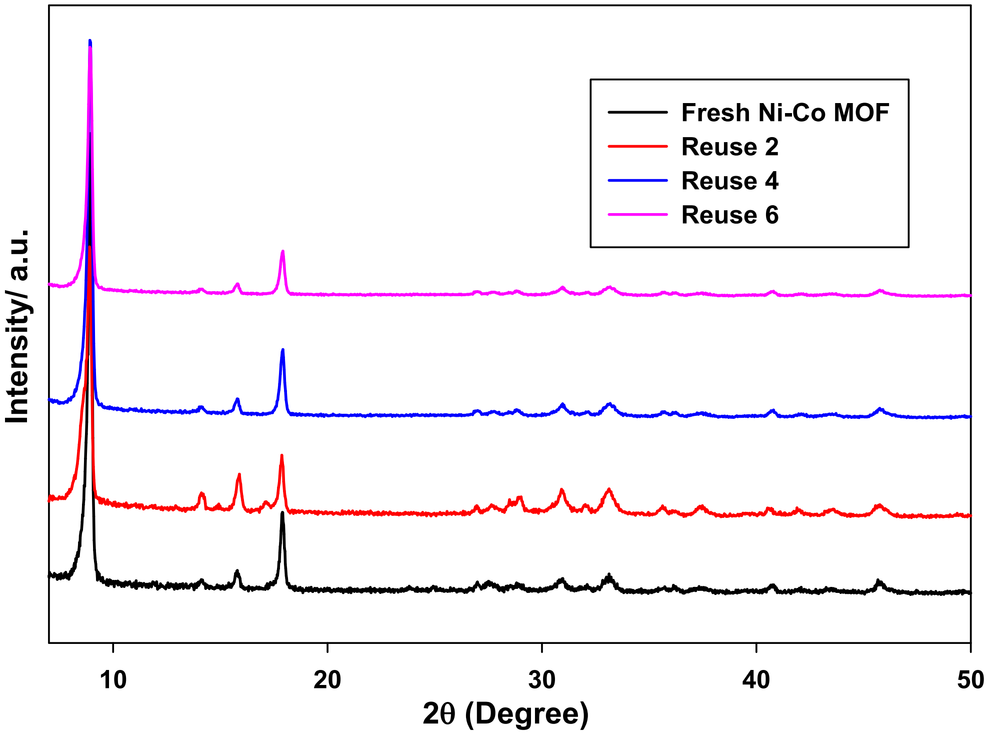

Fig. S14 PXRD patterns of recycled Ni-Co MOF(M).

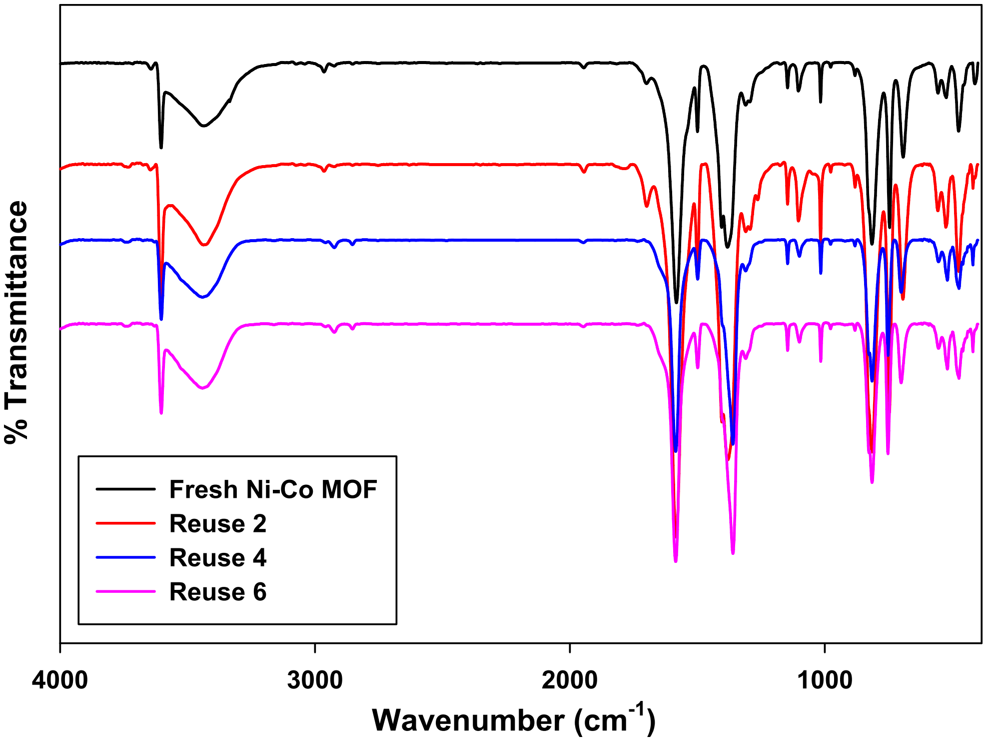

Fig. S15 FT-IR spectra of recycled Ni-Co MOF(M).

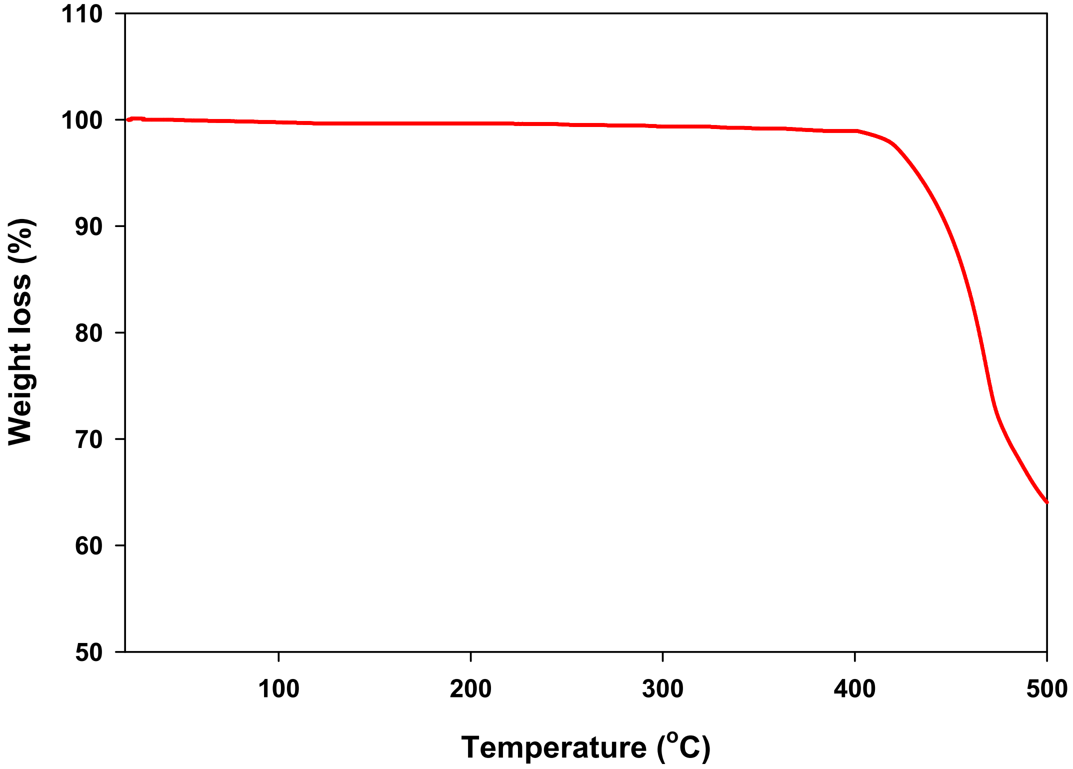

Fig. S16 Thermal gravimetric analysis (TGA) of recycled Ni-Co MOF(M).